

PointIso: Point Cloud Based Deep Learning Model for Detecting Arbitrary-Precision Peptide Features in LC-MS Map through Attention Based Segmentation

Fatema Tuz Zohora¹, M Ziaur Rahman², Ngoc Hieu Tran¹, Lei Xin², Baozhen Shan², and Ming Li^{1,*}

¹David R. Cheriton School of Computer Science, University of Waterloo, Waterloo, ON N2L 3G1, Canada

²Bioinformatics Solutions Inc., Waterloo, ON N2L 6J2, Canada

*mli@uwaterloo.ca

ABSTRACT

A promising technique of discovering disease biomarkers is to measure the relative protein abundance in multiple biofluid samples through liquid chromatography with tandem mass spectrometry (LC-MS/MS) based quantitative proteomics. The key step involves peptide feature detection in LC-MS map, along with its charge and intensity. Existing heuristic algorithms suffer from inaccurate parameters since different settings of the parameters result in significantly different outcomes. Therefore, we propose PointIso, to serve the necessity of an automated system for peptide feature detection that is able to find out the proper parameters itself, and is easily adaptable to different types of datasets. It consists of an attention based scanning step for segmenting the multi-isotopic pattern of peptide features along with charge and a sequence classification step for grouping those isotopes into potential peptide features. PointIso is the first point cloud based, arbitrary-precision deep learning network to address the problem and achieves 98% detection of high quality MS/MS identifications in a benchmark dataset, which is higher than several other widely used algorithms. Besides contributing to the proteomics study, we believe our novel segmentation technique should serve the general image processing domain as well.

Introduction

Deep learning, an emerging branch from machine learning, has exhibited unprecedented performance in a wide range of research areas, including image processing, pattern recognition, natural language processing and many others¹. Deep Learning is accelerating new scientific discoveries not only in core machine learning problems, but also many multidisciplinary sectors, like bioinformatics, autonomous driving, fraud detection, etc. Proteomics is the large scale study of proteins - main workhorses responsible for biological functions and activities in a cell, tissue, or organism. Liquid chromatography coupled with tandem mass spectrometry (LC-MS/MS) based analysis leads the pathway of disease biomarker identification², antibody sequencing³, neoantigen detection⁴, drug discovery and many other clinical research⁵. Since peptide is the building block of protein, there has been significant effort on peptide identification, sequencing, and quantitation. Most of these problems involve pattern recognition and sequence prediction. That is why the popular deep learning models, e.g., convolutional neural network (CNN), recurrent neural network (RNN), etc. are worth applying in proteomics domain as well. Bulik-Sullivan et al.⁴ proposed a deep learning based model EDGE, that shows improved ability to develop neoantigen-targeted immunotherapies for cancer patients using tumor HLA peptide mass spectrometry datasets. Tran et al.⁶ proposed DeepNovo-DIA, a deep learning based de novo peptide sequencing technique. PROSIT is proposed by Gessulat et al.⁷ that offers a proteome-wide prediction of peptide tandem mass spectra by deep learning. Guan et al.⁸ proposed deep learning strategy for the prediction of LC-MS/MS properties of peptides from sequence. AlphaFold⁹, developed by Google's DeepMind, makes significant progress on protein folding, one of the core challenges in biology. We proposed DeepIso¹⁰, that combines recent advances in CNN and RNN to detect peptide features of different charge states, as well as, estimate their intensity. It is the first deep learning based model to address the target problem and should be applicable in protein quantitation and biomarker discovery as well. However, it is a fixed precision model (up to 2 decimal places) and comparatively slower than other competitive tools. But it gave us a good insight on the scope of deep learning in this context. So we make significant improvements in DeepIso and propose PointIso that resolves all those shortages.

Many diseases are fundamentally linked to proteins. Therefore, if we can measure the relative protein abundance between the biofluid samples from healthy person and disease afflicted person, we can identify the proteins which are either diagnostic or prognostic of the disease. Such proteins are called disease biomarkers. The LC-MS/MS based analysis is the current

state-of-the-art technology for protein identification and quantification¹¹. The procedure starts with digesting the protein into smaller peptides by various sequence-specific enzyme, and then the protein sample is passed to the first mass spectrometer (MS), where the peptides are ionized. Output of the first MS is called LC-MS map or MS1 data, that contains the three dimensional peptide features as shown in Figure 1. The three dimensions are: mass-to-charge (m/z or Th), retention time (RT), and intensity (I) of peptide ions in that sample. Each peptide feature consists of multiple isotopes and appears during its elution time (RT range) in the map. The precursor ions (peak intensity isotope in the feature) are further passed to the second MS which generates MS/MS fragmentation spectrum that facilitate the identification of peptide sequence¹², i.e., the amino acid sequence. We have to find the precise peptide feature boundary from LC-MS map, since this is a crucial step for many downstream workflows, e.g., protein quantification, identification of chimeric spectra, biomarker identification, etc.

There has been past attempts of peptide feature detection using several heuristic algorithms whose parameters are set by domain experts through rigorous experiments, and different dataset needs different set of parameters. Its prone to human error since different settings result in significantly different outcomes. Therefore, our target problem is to build up an automated system that learns the parameters itself using the power of deep learning through several layers of neurons by training on appropriate dataset. To be specific, we propose a deep learning based model that detects the peptide feature boundary along with its charge state. Although this resemblance common pattern recognition problems in machine learning, however, there are several reasons what make the peptide feature detection far more challenging than the general cases. For instance, frequent overlapping among the multi-isotope patterns, not always obeying typical conventions, need for filtering out from feature like noisy signals, and hundreds of thousands of peptide features who are comparatively tiny in size as compared to the massive background (RT axis span over 0 to 120 minutes, and m/z axis ranges from 400 to 2000 m/z with resolution as high as up to 4 decimal places). DeepIso¹⁰ shows better performance than other existing heuristics based tools. However, it cannot accept very high resolution input due to using image based CNN, and comparatively slower than other competitive tools because of using classification network in a overlapping sliding window approach for doing the feature segmentation. Therefore, we bring significant changes to overcome these problems and offer PointIso that gives precise boundary information in a time efficient manner and achieves higher percentage of feature detection. In particular, we combine point cloud based deep neural network PointNet¹³ and Dual Attention Network (DANet)¹⁴ to integrate local features with their global dependencies and some context information. Point cloud is a data structure for representing objects using points, e.g., using triplets in a three dimensional environment. Unlike DeepIso where 2D projected image are used for representing 3D peptide features, we adapt PointNet to our context in order to directly process the 3D features. It makes it feasible to accept input data with two or more times higher resolution (arbitrary-precision) than DeepIso and achieves better detection. On the other hand, the original DANet is proposed for finding the correlated objects in the input landscape image for the autonomous driving problem. We take the idea and plug it into the PointNet network to solve boundary value problems during scanning the huge LC-MS map through *non-overlapping* sliding windows, which makes it three times faster than DeepIso. Therefore, PointIso achieves a higher peptide feature detection rate with a faster speed than before.

Our novel concept of attention based scanning of LC-MS map through completely non-overlapping sliding window for peptide feature detection not only leads us to a high feature detection rate in a reasonable running time, but also has the potential to serve the general image processing problems. Besides that, our deep learning model is easily adaptable to new cases by fine tuning through retraining with the misclassified samples. Therefore, we believe our research work discloses new research directions, as well as, makes a notable contribution in accelerating the progress of deep learning in proteomics study.

Results

We explain the intuition of our proposed model using the workflow shown in Figure 1. We see the three dimensional LC-MS map in the upper left corner and PointIso starts with scanning this map by sliding a window along two directions: m/z axis and RT axis. A sliding window is essentially a 3D cube, which can be represented using point cloud. We show a random scanning window in bold black boundary, enclosing two features. This region is further shown in the next image, labeled as 'Zoomed in Simplified View'. Here, two features A and A are shown using red and green boundary. The corresponding point cloud version of this window is shown in the next image, labeled as 'Point Cloud Input'. Here the blue and white points correspond to the features and background points respectively. We also see that PointIso model works through two modules, IsoDetecting in the first step, and IsoGrouping in the second step. So the point cloud input consists of a set of 'N' datapoints which is passed as input to the IsoDetecting module as shown by the arrow sign from the sliding 3D window. IsoDetecting module segments the datapoints as $z = 0$ to 9, where $z=0$ means the respective datapoint is a noise, and $z = 1$ to 9 means the respective datapoint belongs to a feature having charge z . We build this module by incorporating the attention mechanism offered by DANet into the PointNet architecture, in order to support *non-overlapping* sliding windows. IsoDetecting module gives us a list of isotopes of potential features, and are recorded in a hash table. Then in the second step, IsoGrouping module takes those sequences of isotopes (each sequence may have any number of isotopes) and predicts the boundary (first and last isotope) of features. Each sequence may be broken into multiple features or merely predicted as noisy signals. This prediction finally gives us a feature

table that reports the detected peptide features along with the m/z of monoisotope (the first isotope of a feature), charge, RT range of each isotope, and intensity. We can also visualize the final result as shown in the image labeled as ‘Visualize Output’ in Figure 1 (upper right corner).

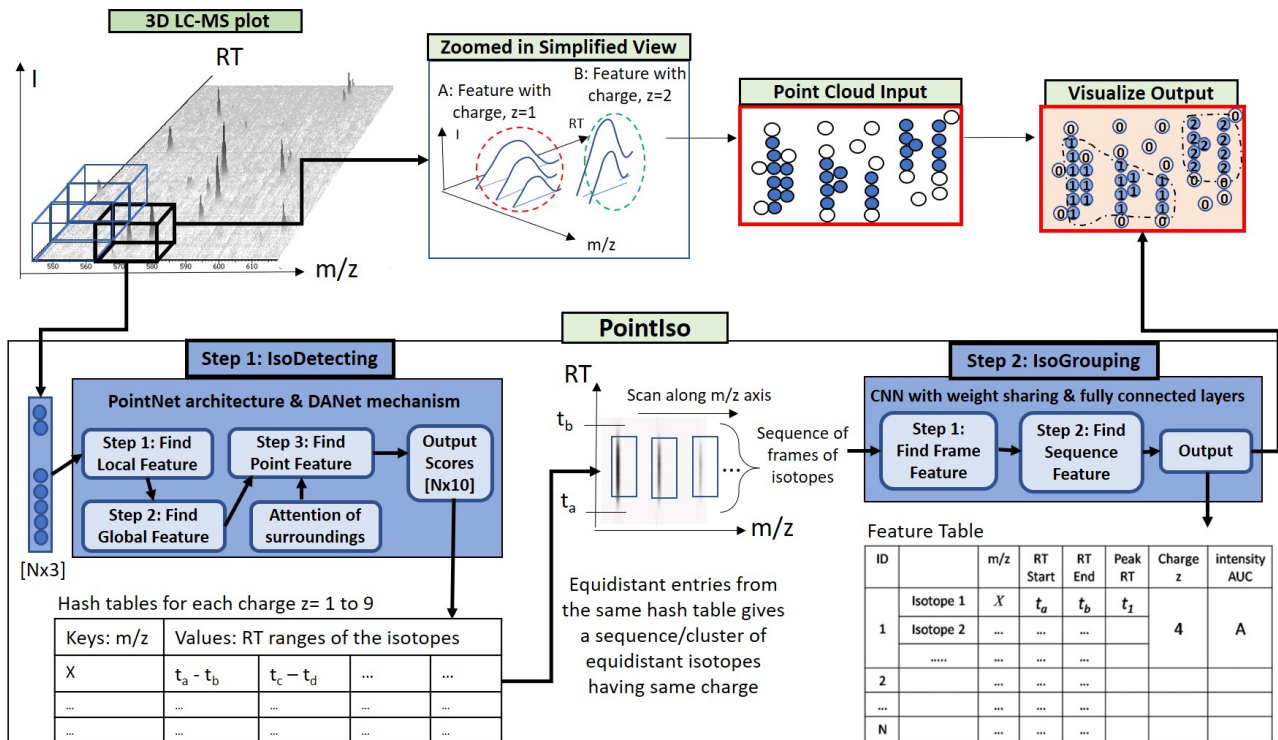


Figure 1. Workflow of our proposed model PointIso to detect peptide features from LC-MS map of protein sample

We downloaded the benchmark dataset from ProteomeXchange (PXD001091) which was prepared by Chawade et al.¹⁵ for data-dependent acquisition (DDA). The samples consist of a long-range dilution series of synthetic peptides (115 peptides from potato and 158 peptides from human) spiked in a background of stable and nonvariable peptides, obtained from *Streptococcus pyogenes* strain SF370¹⁶. Synthetic peptides were spiked into the background at 12 different concentration points resulting 12 samples each having multiple replicates. We obtain LC-MS map from each replicate, totaling 57 LC-MS maps for the experiment.

Training of PointIso

Since we are using supervised learning approach, we need labeled data for training. Human annotation of peptide features is out of scope due to gigapixel size of the LC-MS maps¹⁷. Therefore, we match the feature lists produced by MaxQuant 1.6.3.3 and Dinosaur 1.1.3 with a tolerance of 10 ppm m/z and 0.03 RT and take the common set as the training samples. In PointIso we also need the precise boundary information (i.e., RT time range and m/z value of each isotopes of the features) which is not generated for the users in MaxQuant. Therefore we use Dinosaurs for that information. The IsoDetecting and IsoGrouping modules are trained separately using suitable training data. In order to generate training samples for IsoDetecting module, we place scanning window over the features and cut the region along with surrounding area. The total number of features available from each charge state is presented in Table 1. Input resolution of our dataset is up to 4 decimal places along m/z axis (whereas DeepIso accepts only 2 digits after the decimal point). For training the IsoGrouping module, we cut sequence of frames (each frame holding an isotopic trace) from these peptide features. The detailed procedure and training results are discussed later in Method section. We apply $k = 3$ fold cross validation¹⁸ technique to evaluate our proposed model.

Class (charge state)	1	2	3	4	5	6	7	8	9
Peptide Features	163,038	863,050	428,909	29,183	1,503	653	179	236	233

Table 1. Class distribution of peptide features in our dataset consisting of 57 LC-MS maps.

Performance Evaluation of PointIso

We run MASCOT 2.5.1 to generate the list of MS/MS identified peptides and the identifications with peptide score > 25 (ranges approximately from 0.01 to 150) are considered as high confidence identifications⁵. For performance evaluation, we compare the percentage of high confidence MS/MS peptide identifications matched with the peptide feature list produced by our algorithm and some other popular algorithms. Since the identified peptides must exist in LC-MS maps, therefore, the more we detect features corresponding to them, the better the performance^{5,17,19,20}. The other tools used for comparison are MaxQuant 1.6.17.0²¹, OpenMS 2.4.0²⁰, Dinosaur 1.2.0²², and PEAKS Studio X²³. The benchmark dataset is prepared by Chawade et al.¹⁵, and we use the MaxQuant parameters published by them. For Dinosaur, default parameters mentioned at their github repository (<https://github.com/fickludd/dinosaur>) are used. For OpenMS, we use the python binding pyOpenMS^{20,24} and follow the centroided technique explained in the documentation. For all of the feature detection algorithms, we set the range of charge state 1 to 9 (or the maximum charge supported by the tool).

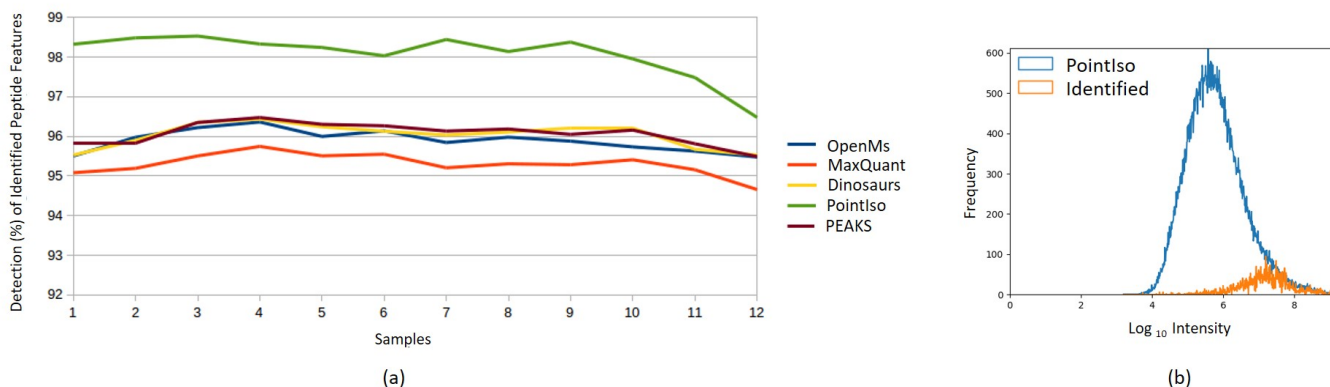


Figure 2. (a) Detection percentage of identified peptide features by different tools for 12 samples, each having different concentration. (b) Intensity distribution of peptide features detected by PointIso (blue) and identified by database search (orange). We see that the distribution of identified features is wedged into the high intensity tail of the distribution of detected peptide features, because only high intensity features are selected for fragmentation.

Percentage of Identified Peptide Features Detected by PointIso

We show the plot of detection percentage of high confidence MS/MS identifications with error tolerance of 0.01 m/z and 0.2 minute peak RT^{10,15,22} for 12 samples by different algorithms in Figure 2 (a). We see that the PointIso has significantly higher detection rate for all the samples and on average 98.01% as presented in the first row of Table 2 (entire result can be found in Supplementary Table S3). If we just match all the MS/MS identifications (any score) with the peptide features, our algorithm consistently provides higher detection rate than other tools as presented in the second row. Multiple MS/MS fragments coming from different peptide features can be matched with the same peptide sequence during the database search. Unlike the experiments with DeepIso, here we treat those MS/MS identifications as different entities if their m/z and peak RT values are significantly different, as it seems more appropriate. We further want to emphasize the fact that, although the model is trained on sample features from certain concentration (e.g., sample 5, 6, 7, 8), but it can detect features having higher or lower concentration as well (e.g., sample 1 to 4, and 9 to 12). It implies that the model can well generalize the peptide feature properties irrespective of peptide intensities seen during training time.

Matching Criteria	MaxQuant	OpenMS	Dinosaur	Peaks	DeepIso	PointIso
MS/MS identifications with high confidence score	95.24%	95.86%	96.01%	95.66%	96.05%	98.01%
All MS/MS identifications	93.73%	94.03%	94.90%	94.82%	94.10%	96.98%

Table 2. Percentage of MS/MS identifications matched by feature list produced by different algorithms.

Quality of Peptide Features Detected by PointIso

Next we discuss our observation on the peptide features detected by PointIso, but non-identified by database search. The DDA mode ensures that the most abundant peptides are fragmented and thus only those are tempted for identification. However, the real number of peptide species eluted in a single LC run can be over 100,000²⁵. During biomarker identification through

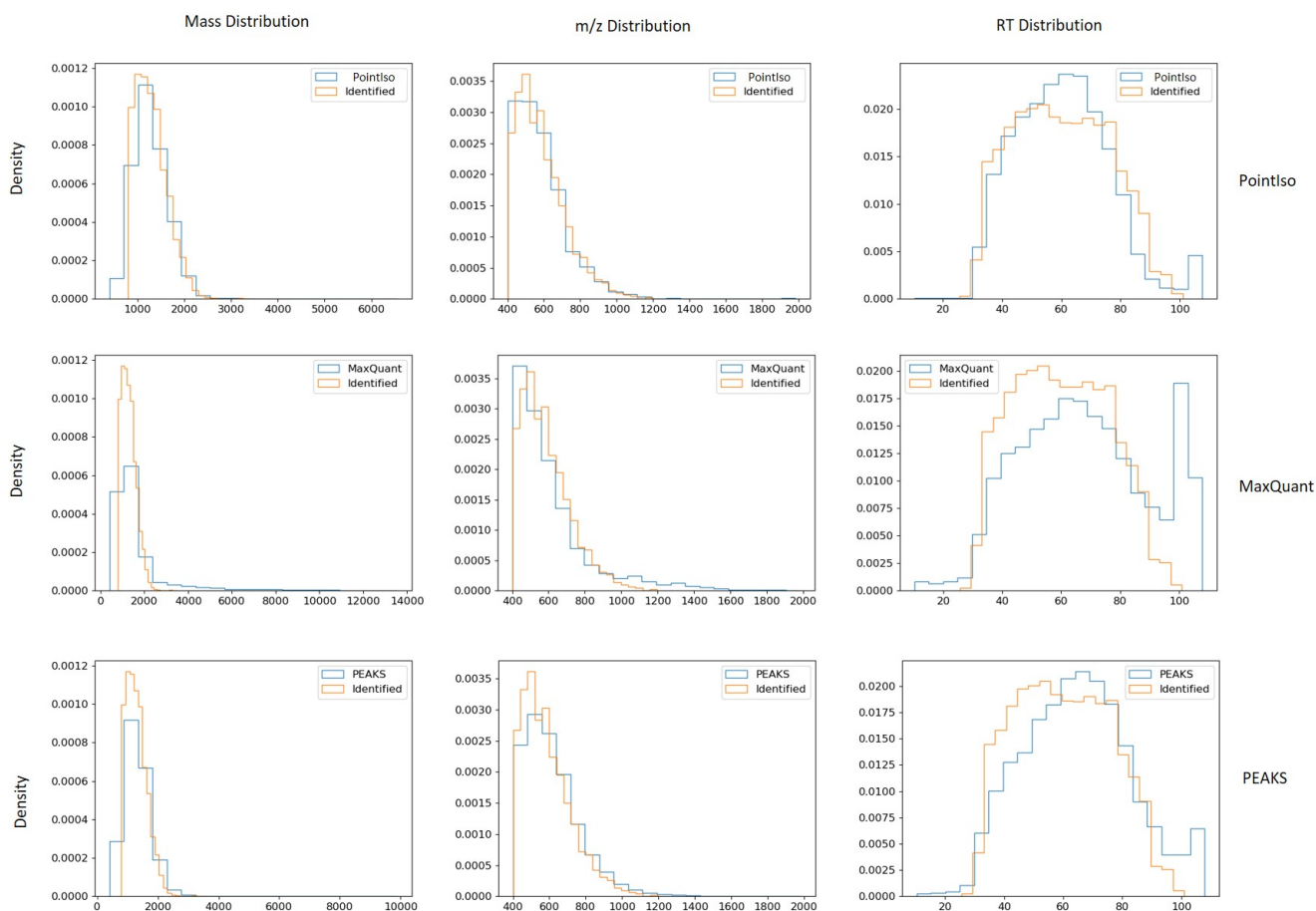


Figure 3. Comparison of mass, m/z and RT distribution of detected features (blue) and identified features (orange) for different tools. First, second, and third rows of plots are representing the result for PointIso, MaxQuant, and PEAKS respectively (distributions for other tools are included in Supplementary Figure S2). The orange distributions remain same along the column since its representing the identified peptides. Plots in the first column shows that all algorithms might have some false positives below 1000 Da mass, but the rate is lowest for PointIso. MaxQuant may have some false positives above 2000 Da as well. Then the second column is representing the distribution of m/z . Again, MaxQuant might have some false positives in the higher range of m/z . Finally, the third column is presenting the distribution of RT and all the tools have a probability of detecting false positives above 100 minute RT, but that rate is lowest for PointIso. Besides that, both MaxQuant and PEAKS might report some false positives below 30 minute RT. For PointIso, the histograms of detected features (blue) are showing good alignment with the histograms of identified features (orange), and implies strong evidence for being true features

relative protein quantification, it is desirable to assess the identity of those remaining peptide features which do not readily match with any MS/MS identification but shows significant abundance change among multiple samples. This is done by performing post-annotation of the remaining peptide features through targeted MS/MS². That is why we wanted to verify whether the PointIso detected but non-identified features are potential peptide features or not. Please note that the typical statistical methods for finding the false positive rate is not applicable here due to the absence of ground truth about the existence of those non-identified peptide features^{10,17}. However, one reliable technique is to observe their intensity distribution which should be log normal and if there are many false positives then there will be multiple peaks in the distribution²⁵. We present the intensity distribution of the detected features by PointIso in an LC-MS/MS run in Figure 2(b) which is quite well behaved. Besides this, we also investigated the physicochemical properties of the two populations (blue and orange) as shown in Figure 3. It demonstrates that the PointIso detected peptide-like features indeed represent peptides²⁵. Therefore, we state that PointIso has low false positive rate besides having high detection rate of identified peptides.

Peptide Feature Intensity Calculation by PointIso

Next we would like to verify the correctness of peptide feature intensity calculation by our model. The perfectness of peptide feature intensity depends on whether the bell shaped signals are detected nicely or not. We report the Pearson correlation coefficient of the peptide feature intensity, calculated as Area Under the Curve (AUC), between PointIso and other existing algorithms in Table 3. It appears that our algorithm has a good linear correlation with other existing algorithms, which implies that the peptides which are measured differentially among different samples by other tools will also be reported differentially by PointIso. Thus it validates the peptide feature intensity calculation by our model.

	Dinosaur	MaxQuant	OpenMS	PEAKS
PointIso	89.88%	95.31%	93.76%	88.93%

Table 3. Pearson correlation coefficient of the peptide feature intensity between PointIso and other tools.

Time Requirement of PointIso

Total time of scanning LC-MS map by IsoDetecting module and IsoGrouping module is considered as the running time of PointIso model. The running time of different algorithms along with the platforms used in our experiment is presented in Table 4. It appears that our PointIso model is about three times faster than DeepIso and has a comparable running time with most of the existing tools. Although PEAKS is much time efficient than all other tools, we believe PointIso can be made faster by using multiple powerful GPU machines in parallel.

Platform	Processor: Intel Core i7, 4 cores OS: Windows 10 for running the applications			Processor: Intel(R) Xeon(R) Gold 6134 CPU, NVIDIA Tesla OS: Ubuntu 16.04.5 LTS for running the python scripts		
Algorithms	PEAKS	Dinosaur	MaxQuant	PointIso	DeepIso	OpenMS
Running Time	8 minutes	15 minutes	30 minutes	30 minutes	1 hour and 40 minutes	2 hours and 50 minutes

Table 4. Approximated running time of different algorithms. Here the platform used for OpenMS, DeepIso and PointIso did not have support for running Windows application of PEAKS, MaxQuant, and Dinosaur. So we used different machine for running those.

Finally, we want to emphasize the fact that, our PointIso is able to learn the general peptide feature properties irrespective of the concentration of protein samples provided during the training. Because the twelve LC-MS maps in the dataset comes from three different range of protein concentration: low, medium, and high. We train over one range and run the test on two other ranges. The average detection results are already discussed and we see that the PointIso consistently provides higher detection rate. It implies that, once we train a model on a protein sample, the same model should be applicable to all other protein samples from the same or other close species without further training. This should make PointIso more appealing in the practical sectors.

Discussion

We propose PointIso, a deep learning based model that discovers the important characteristics of peptide feature by proper training on vast amount of available LC-MS data. Other heuristic algorithms have to set different parameters, e.g., number of scans to be considered as feature, centroiding parameters, theoretical formulas for grouping together the isotopes, and also data dependant parameters for noise removal and other preprocessing steps. On the other hand, PointIso does not rely on manual input of these parameters anymore and systematically learns all the necessary parameters itself. We will first demonstrate the justification of different design strategies performed. Then we will discuss some prospective research directions. We show a complete breakdown of different developmental stages in Table 5, which is referred in different sections of the following discussion.

Point Cloud Representation of IsoDetecting Module with Weighted Cross Entropy Loss

In DeepIso, IsoDetecting module process the 2D image representation of LC-MS map by sliding a window pixel by pixel, and producing a output $z = 0$ to 9 at each step using classification network, depending on whether there is a feature aligned with the window or not. Accepting higher resolution input is feasible if we formulate IsoDetecting network as a segmentation network so that one scanning window can predict all datapoints in it at a time. Now, a scanning window covers 15 RT scans and 2.0 m/z having resolution of up to four decimal points. With point cloud representation it has to predict the label of about 5000 points only (the 95th percentile of the number of datapoints in all the sample scanning windows), whereas it needs to predict 300,000

Model	Matching with MS/MS identified peptides
Initial model	65%
Bi-directional 2D RNN	72%
Dual attention mechanism	94%
Retraining of IsoDetecting module with long RT range	95.5 %
Increasing resolution from 0.01 m/z to 0.0001 m/z	97%
Retraining using features detected with wrong charge by IsoDetecting module	98.22%
New architecture of IsoGrouping module	99.55%
Fine tuning with feature like noises	98.52%

Table 5. Performance of PointIso in different developmental stages (based on validation dataset).

pixels with 2D image representation ($15 \times \frac{2.0}{0.0001} = 300,000$), where most of the points will be blank. So image representation makes the segmentation problem unnecessarily voluminous. Therefore to support higher resolution compatibility at a faster speed, we move from image to point cloud representation of datapoints. There are also other literature, e.g., DeepNovoV2²⁶, which switched to point cloud representation for supporting higher resolution data like us.

Unlike DeepIso, we had to deal with highly class-imbalanced problem with this new representation of IsoDetecting module. Only 20% of 5000 input datapoints are positive and all other datapoints are noisy signals or just have zero intensity. However, a positive datapoint might also be recorded as zero or low intensity point due to instrumental noise. So we cannot just disregard those datapoints. Therefore, we use class weights while calculating cross entropy loss so that both the positive and negative datapoints are learnt well. We use class weights decided based on the distribution per sample, since it tries to achieve well balanced class sensitivity according to our experiments (included in Supplementary Note A). This initial model was able to achieve about 65% matching with the peptide identifications as shown in Table 5. Therefore we were in need of further investigations for the improvement which are discussed in next section.

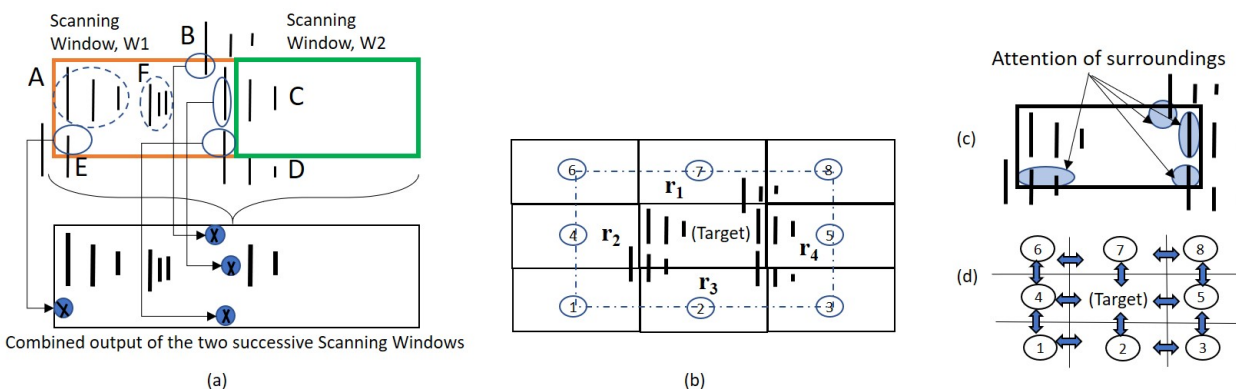


Figure 4. (a) We show two successive and non-overlapping scanning windows, W1 and W2, and six features: A, B, C, D, E, and F. We show the combined output of the two successive scanning windows in the bottom image. Feature A and F are fully contained within W1. Therefore, all of its isotopic signals are correctly detected, as shown in the combined output. However, for each of other four features, W1 sees partial traces shown by small circles in the upper image. Without any background knowledge, those traces are not adequate for deciding whether they belong to real features or merely noisy traces. We mark the isotopes by cross sign which are not detected. The second window W2 detects two isotopes of feature C. But the system missed the monoisotope of feature C, which is treated as missing the feature as a whole. (b) Surrounding regions of a target window. (c) Attention of surrounding regions over the datapoints of target window. (d) 2D bi-directional RNN to flow the surrounding information towards the target window in center.

Attention Mechanism

Next, we discuss the reason of using attention mechanism with segmentation network of IsoDetecting module. In a random scenario feature can spread over multiple windows, and simply using segmentation network without any surrounding knowledge will cause missing of the features, e.g., feature C, as illustrated in Figure 4(a). It also fails to compute total abundance of features perfectly, since its missing trailing regions of features like B, D, and E. To overcome this problem we have to

Experiment Category	z=0	z=1	z=2	z=3	z=4
Sliding window with 50% overlapping	86%	50%	72%	57%	36%
Skiplink inserted in above model	85%	56%	76%	66%	41%
Bi-directional 2D RNN	85%	51%	77%	67%	49%
Attention mechanism	84%	62%	85%	71%	50%
Attention mechanism with higher resolution	90%	64%	85%	81%	61%

Table 6. Different techniques of absorbing surrounding information and corresponding class sensitivity of IsoDetecting module. We define the class sensitivity of a scanning window as the number of datapoints from class z (0 to 9) detected correctly out of total number of datapoints in a scanning window. To evaluate candidate solutions we use the class sensitivity of high abundant features (charge $z = 1, 2, 3$, and 4) in a *average case* scenario. Average case means the scanning window might contain any number of features, they may appear at any location of the window, they might be partially or fully seen, and might be overlapping as well. We see that the DANet inspired attention based mechanism works better than other techniques.

incorporate surrounding knowledge while segmenting the datapoints of a target window, i.e., $W1$ in Figure 4(a). According to our experiments, we find that the regions r_1, r_2, r_3 , and r_4 in Figure 4 (b) are actually playing the key role in detecting the traces inside target window. Our experimental results with three different criteria: 50% overlapping of scanning window, Bi-directional 2D RNN (Figure 4 (d)), and the attention mechanism (Figure 4 (c)) inspired by DANet are presented in Table 6. Besides that, we also had a visual verification about whether the partially seen peptide features are properly detected or not as presented in Figure 5 (a) and (b). Since PointNet segmentation network combined with DANet works better than other techniques, we choose this to develop our IsoDetecting module.

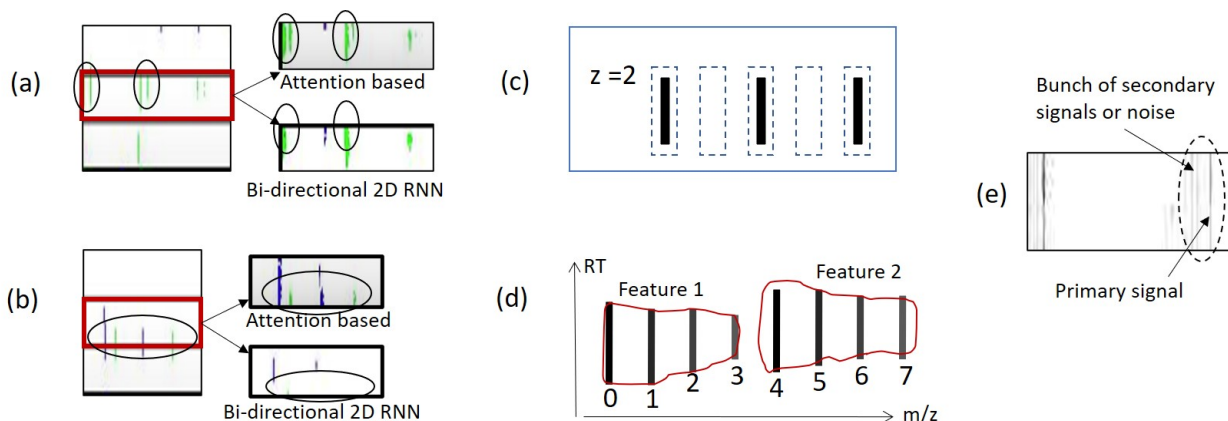


Figure 5. (a) and (b) are showing the comparison between attention based mechanism and bi-directional 2D RNN. The Red rectangle is showing the target window. Detection by attention mechanism and bi-directional two dimensional RNN for each target window are shown next to it, pointed by arrow signs. We see that attention mechanism works better in separating closely residing features in (a), and detecting partially seen features in (b). (c) When isotope lists are passed to the IsoGrouping module with wrong frames (dotted rectangles) due to the wrong charge ($z = 4$) detected by IsoDetecting step, it results in discarding this whole group of frames as a noise due to the inconsistency (blank frames) observed. (d) Adjacent feature problem. (e) Feature like noisy signals

Upgrading IsoGrouping Module

IsoDetecting module outputs the isotope list with m/z resolution of up to 4 decimal places, but IsoGrouping module does not need that much high resolution to group together the potential isotopes into a feature. Therefore, we use a resolution degrading approach before passing the isotope lists to IsoGrouping module. But we ensure that the isotopes who merge together in lower resolution are kept in separate list and thus passed to IsoGrouping module separately. This resolves the problem of missing features merged in lower resolution, one of the key problems of DeepIso. Besides that, in that model each frame of the input sequence covers a wide range of m/z value. As a result, each frame holds an isotopic signal along with its background. But in PointIso, we filter out the signal area from background, based on the boundary information provided by IsoDetecting module. So the background of input frames are mostly blank, and IsoGrouping module can see the bell curve better than before. As a result we can get rid of the attention gate in this module to keep it simpler. Another change is, instead of using RNN layer to

process frames of the sequence one at a time, we process five frames at a time using a network consisting of CNN and fully connected layers through weight sharing. We observe that it results in better prediction at the output layer. Besides that, we incorporate Area Under the Curve (AUC) of isotopic signal as context information through embedding which reduces the uncertainty during class prediction. The charge, detected in previous step is fed into the network through a scaling gate (neuron) which helps in proper grouping as well. The final architecture of IsoGrouping module is quite different and presented later in Method section. It improves the feature detection by about 1.5%, as presented in the seventh row of Table 5.

Fine Tuning Using Misclassified Features

Retraining the primary model by feeding back the misclassified data played an essential role in overall improvement. We applied this approach in learning four particular cases. First, some features having very long RT range were not detected or broken into multiple features by IsoDetecting module. Therefore, fine tuning the model with such samples improves the detection rate by about 2% (fourth row in Table 5). Second, IsoDetecting module was predicting wrong charge for the features like 'F' in Figure 4 (a), which appears in the middle region of the scanning window, i.e., not aligned with the scanning window. As a result, wrong set of frames are passed to the IsoGrouping module, as shown in Figure 5 (c). This causes complete rejection of the feature by IsoGrouping module, and we miss a feature although it was detected in the first module. So, retraining the IsoDetecting module using such samples improves the detection rate by about 1.5% (sixth row in Table 5). Third, adjacent features as shown in Figure 5(d) were not correctly separated by IsoGrouping module. Here, both features have same charge, same or very close RT value at peak intensity point, and the distance between the two features along m/z axis is equal to the distance between their own isotopes. Fine tuning IsoGrouping module with such samples resolves this problem. Finally, we fine tune the model with feature like noisy or secondary signals (e.g., Figure 5 (e)) which appear very close to the main isotopic signal. Although PointIso reports 99.55% detection of identified peptides without this fine tuning, but it also reports multiple features for basically the same peptide feature. After training with such samples the problem is solved with 98.52% detection of identified peptides (discussed further in the Supplementary Note C). It should be an interesting research scope to see if we can solve this problem without reduction in detection percentage. Besides that, we believe the necessity of this step also depends on the dataset and the mass spectrometer used. Because high resolution mass spectrometers usually produce narrower signals without those secondary peaks, thus we might avoid this step and obtain over 99% detection.

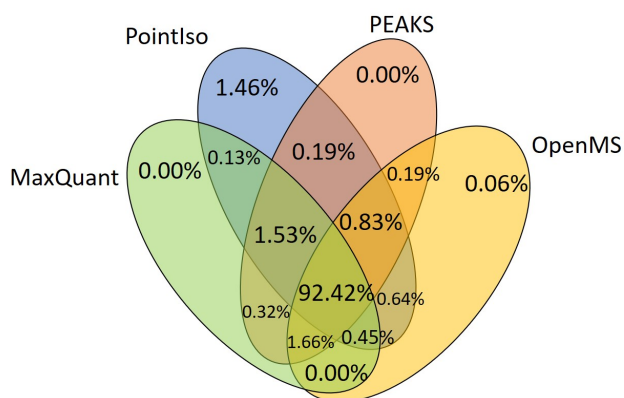


Figure 6. Venn diagram of identified peptide features detected by different algorithms.

Observations on Peptide Features Exclusively Detected by PointIso

We present the Venn diagram of identified peptide features detected by different algorithms in Figure 6 (we show four algorithms to keep the Venn diagram simple). We visually inspected all the features which are detected by PointIso only. We found that the features whose peaks are very close to each other along RT axis, are sometimes merged into one in other tools, e.g., Figure 7 (a), but separated perfectly by PointIso. Similarly, the monoisotope might be missed sometimes by other tools as shown in Figure 7(b). Here, the feature A and C are detected by PointIso. But other tools detect A, and instead of C they report B by mistake, missing the monoisotope (merged with A). Very closely residing and overlapping features, like feature C in Figure 7 (d) are sometimes missed by other tools as well, although detected by PointIso. Besides these, PointIso can detect features even if the signals are not recorded perfectly as Figure 7(c), which are sometimes discarded by other algorithms.

Finally, we refer to the fact that, although we have prepared the training data by taking the common set of Dinosaur and MaxQuant in order to replace human annotators, but the outcome of PointIso is quite different than those algorithms. Because

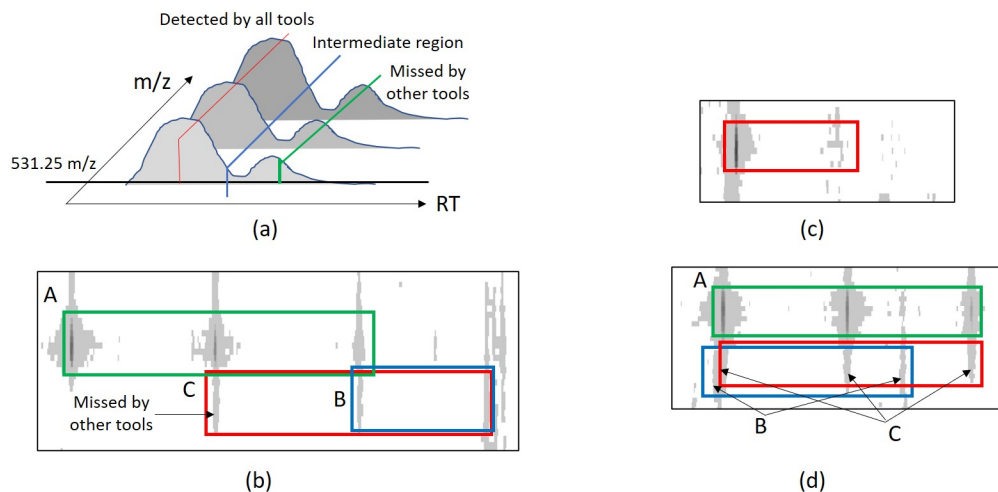


Figure 7. Observations on peptide features detected by only PointIso. (a) Peaks connected by red line are detected as a peptide feature by all algorithms. However, the feature having lower peak, connected by green line, is missed by other tools. Because they have the same m/z as the one with higher peak. Therefore, most of the tools merge it with the bigger one during pre-processing steps. (b) Monoisotope of the feature enclosed in red rectangle is missed by other tools due to merging with A. But PointIso detected both feature A and C. (c) Features with broken signals are detected by our model. (d) Very closely residing and overlapping features, like feature in blue and red rectangles are sometimes missed by other tools as well, although detected by PointIso.

deep learning network learns the required parameters by stochastic gradient descent through several layers of neurons and backpropagating the prediction errors, a completely different technique than all the existing heuristic methods. That is why PointIso achieves higher detection rate than others. Some appealing future works should involve plugging in PointIso in the downstream workflow of peptide quantification, identification of chimeric spectra, and disease biomarker identification. Extending this model for Intact Mass analysis might also be another important research direction. Also it will be interesting to see how the attention based non-overlapping sliding window approach performs in general object segmentation problems. We are looking forward to these research opportunities in the future.

Methods

Our model runs the processing on raw LC-MS map which is obtained in .ms1 format using the ProteoWizerd 3.0.18171²⁷. Then we read the file and convert it to a pointcloud based hash table where RT scans are used as keys and (m/z , intensity) are inserted in a sorted order under those keys. Therefore we have the datapoints saved as triplets (RT, m/z , intensity) in the hash table.

Step 1: Scanning of LC-MS map by IsoDetecting module to detect isotopes

Our network scans the 3D LC-MS plot using non-overlapping sliding window having dimension $2.0 m/z$, 15 RT scan, and covering full intensity range, as already presented in Figure 1. The intensities are real numbers scaled between 0 to 255. Here the objects, i.e., peptide features are to be separated from background. Background may contain feature like noisy signals and peptide features are frequently overlapped with each other. So the target is to label each datapoint represented by triplet (RT, m/z , intensity) with its class. The class is either charge $z = 1$ to 9 (positive) if the datapoint belongs to a feature having that charge, or $z = 0$ if that datapoint comes from background or noise. Each window sees a point cloud which is essentially a set of points, or triplet (RT, m/z , intensity). This is passed through a PointNet architecture as shown in Figure 8. In order to properly segment peptide features spreading over multiple sliding windows, we adapt the DANet¹⁴ and plug into our model to find attention or influence of four surrounding regions (Figure 4 (b)) over the target window datapoints. We present a flowchart in Figure 9, showing the calculation of attention coming from the surrounding regions. The detailed explanation of this flowchart is provided in Supplementary Method A.

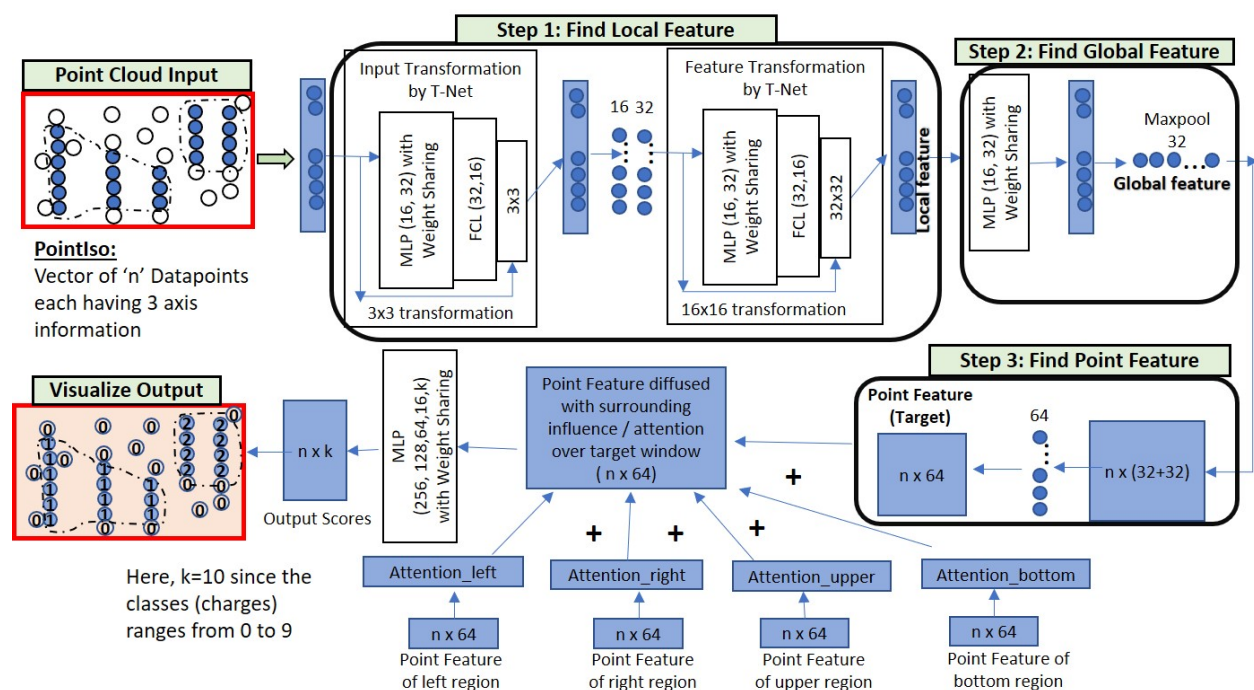


Figure 8. Network of IsoDetecting module. This network goes through three steps, finding the local features, global features and point features respectively of the given target window. The number of layers and neurons in the Multiple Perceptron Layers (MLP) and Fully Connected Layers (FCL) are determined by experiments and mentioned in the figure. Point features of target window are then diffused with features of surrounding regions based on their attention or influence over target window (calculation of *Attention_left* and others are shown in next figure). Finally the diffused features are passed through four MLP and softmax layer at the output provides the final segmentation result.

We can divide the LC-MS map along m/z axis into sections of equal ranges and process multiple sections in parallel to make the process time efficient. We keep nine hash tables for recording the detection coordinates (RT, m/z) of features from nine classes ($z = 1$ to 9) during the scanning. The m/z values of the isotopes are used as the key of these hash tables, and the RT ranges of the isotopes in a feature are inserted as values under these keys as shown in the block diagram of Figure 1. Since the detection of wider isotopes may span over a range of points along m/z axis, we take their weighted average to select specific m/z of an isotope.

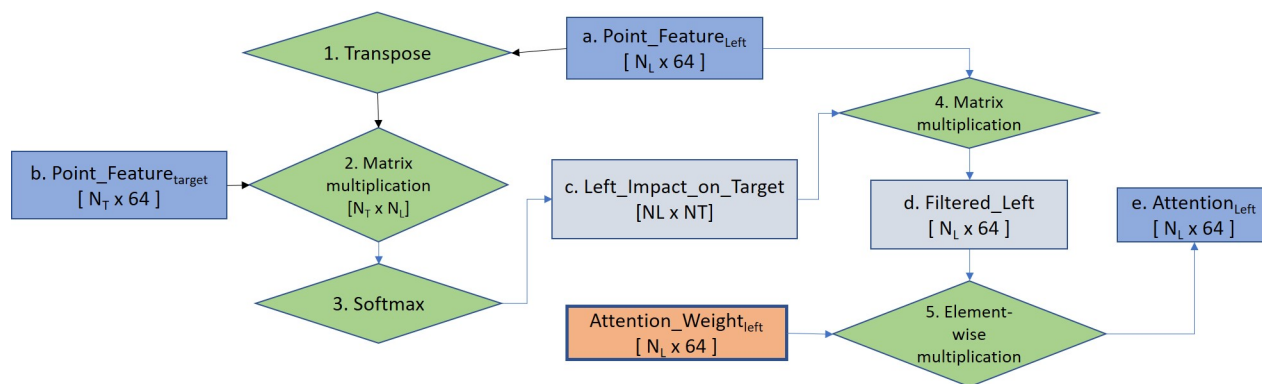


Figure 9. Flowchart of attention calculation in IsoDetecting module. This particular flowchart is intended to find out the attention or impact of left region over the datapoints of target window. Exactly similar approach is followed for other surrounding regions as well and finally all are diffused with the *point_features_target* by addition.

Training Procedure of IsoDetecting module

IsoDetecting module is supposed to learn some basic properties of peptide feature (provided in Supplementary Note D), besides many other hidden characteristics from the training data. Each sample consists of a target window and its four surrounding regions. As already mentioned, we select the common list of peptide features provided by MaxQuant and Dinosaurs, to generate the positive samples. We slide the scanning window over the feature and its surrounding region so that we can generate samples holding peptide features in different locations of the target window, along with its surrounding areas. Similarly we choose some areas containing only noises of different intensities, feature like noisy signals, and completely blank areas as well. We call them negative samples. We see the total number of samples used for training in Table 7. Also note that, unlike DeepIso, IsoDetecting module is segmentation network here. As a result it has to classify each datapoint in a sample. One sample window prepared from feature having charge ‘2’ might contain features with other charges and IsoDetecting module has to classify all those datapoints enclosed by that sample window. Therefore, the class sensitivity is actually impacted by the total amount of datapoints having that class, taking account *all* the training samples. So we have included a column label as ‘Total Datapoints’ in the table.

Class (z)	Training		Validation	
	Total Datapoints	Total Samples	Total Datapoints	Total Samples
0	544,014,927	40,502	22,100,416	10,138
1	3,648,512	37,924	167,671	1,282
2	28,633,707	152,148	1,731,244	8,902
3	19,021,011	91,542	1,033,477	4,485
4	2,998,905	25,526	77,534	281
5	3,526,031	22,134	3,032	13
6	431,139	7,721	606	5
7	30,145	4,472	319	4
8	18,144	8,706	48	3
9	17,310	3,429	227	2

Table 7. Amount of samples for training and validation. Because of inadequate training data for features with charge states 5 to 9 as presented in Table 1, we had to apply data oversampling and augmentation in order to increase training samples from these classes. Amount of samples from class 0 depends on our choice. We chose the amount so that total datapoints from this class is higher than others, because the LC-MS map is very sparse. The validation set does not contain any duplicated data and there is no overlapping between validation dataset and training dataset.

The average sensitivity of the trained model on training set and validation set are provided in Table 8. We use minibatch size of 8 during the training, because the network already takes about 15 GB GPU Memory due to the sophisticated architecture. We use ‘NAdam’ stochastic optimization²⁸ with initial learning rate of 0.001. If we do not observe any significant drop in the validation loss for about 5 epochs, we decrease the learning rate by half. The model converges within about 100 epochs. We use sparse softmax cross entropy as error function at the output layer. Besides that, we apply the class weights as already

mentioned in the Discussion section and is elaborated in supplementary material.

Class (z)	Training		Validation	
	Sensitivity-Average (%)	Sensitivity-Best (%)	Sensitivity-Average (%)	Sensitivity-Best (%)
0	88.48	30.0	88.48	38.69
1	57.59	91.0	61.54	99.28
2	76.90	97.0	82.98	98.40
3	75.08	94.75	79.42	96.05
4	64.78	94.24	52.80	97.33
5	88.57	94.21	58.74	100
6	60.73	82.5	15.68	70.56
7	40.12	60	10.03	70.78
8	4.07	10	3.0	10
9	4.50	8	2.01	15

Table 8. Class sensitivity of IsoDetecting module. We show two cases, average and best case in terms of feature detection ability. Best case occurs when the feature is left aligned with the scanning window boundary, e.g., feature ‘A’ in Figure 4 (a). Average case means the scanning window might contain any number of features, they may appear at any location of the window, they might be partially or fully seen, and might be overlapping as well. Due to the lack of variance in training data for charge states 6 to 9, the model’s validation sensitivity does not go up high for these classes. However, since most of the peptide features appear with charge states < 6 , lower sensitivity for them does not impact the overall performance. The validation set does not contain any duplicated data and there is no overlapping between validation dataset and training dataset.

Step 2: Scanning of LC-MS Map by IsoGrouping Module to Report Peptide Feature

There are four major differences in IsoDetecting and IsoGrouping modules. First, the IsoDetecting module scans the LC-MS map along both the RT and m/z axis, whereas IsoGrouping module scans left to right, i.e., only along the m/z axis. Second, IsoDetecting network is a point cloud based network, whereas the IsoGrouping network is an image based network. Third, IsoGrouping module performs a sequence classification task that generates one output after seeing through 5 consecutive frames, unlike IsoDetecting module which segments the datapoints of the input frame. Last, IsoDetecting module accepts very high resolution m/z values (up to 4 decimal place), but IsoGrouping works on comparatively lower resolution m/z values (up to 2 decimal place), because it does not need such higher resolution to group the isotopes into features.

IsoDetecting module provides us a list of isotopes. Equidistant isotopes having same charge are grouped into a cluster or sequence. Then those sequences of isotopes are passed to the IsoGrouping module. Unlike DeepIso, we do not pass the isotopes directly to the second module, because here the input resolution is different in two modules. Therefore we apply a resolution degradation technique that filters out the region of isotope (as suggested by IsoDetecting module) from the background, presents it in lower resolution, and then pass it to the IsoGrouping module. The detailed procedure is provided in the Supplementary Method B.

Our proposed network for IsoGrouping module is illustrated in Figure 10. It may break each sequence into multiple features, or report one feature consisting of the whole sequence of isotopes, or even report that sequence as merely noise. It works on a sequence of isotopes in multiple rounds. Each round process five consecutive isotopes at a time. The output is $i = 0$ to 4, where, $i = 0$ means that no feature starts at the first frame, so skip it. Output $i = 1$ to 4 means, there is a feature starting in the first frame, and it ends at $(i + 1)^{th}$ frame. If output $i = 4$, it means that the feature might have more than 5 isotopes. Those can be found by overlapping rounds. A step by step explanation of the scanning procedure with figure is provided in Supplementary Method C.

Training Procedure of IsoGrouping module

Usually monoisotope’s intensity is the highest among the other isotopes in a feature and dominates the total intensity of the feature. This property should be learnt by IsoGrouping module. We prepare the positive samples by generating a sequence of 5 frames for each peptide feature, where the sequence starts at the first isotope of the respective feature. Each frame has dimension $[15 \times 3]$, covering 15 scans along RT axis and 3 units along the m/z axis. We filter out the isotopic signal from background by taking the intensity within range 2 ppm before and after the peak intensity m/z value, and 7 scans before and after the peak intensity RT value. The signal is left aligned with the frame. Each sequence is labeled by the frame index holding the last isotope of the feature (indexing starts from 0). Minimum number of isotopes in a feature is 2, i.e., label is 1. If the feature has equal of more than 5 isotopes, label is 4. We generate negative samples by cutting some sequences from the noisy

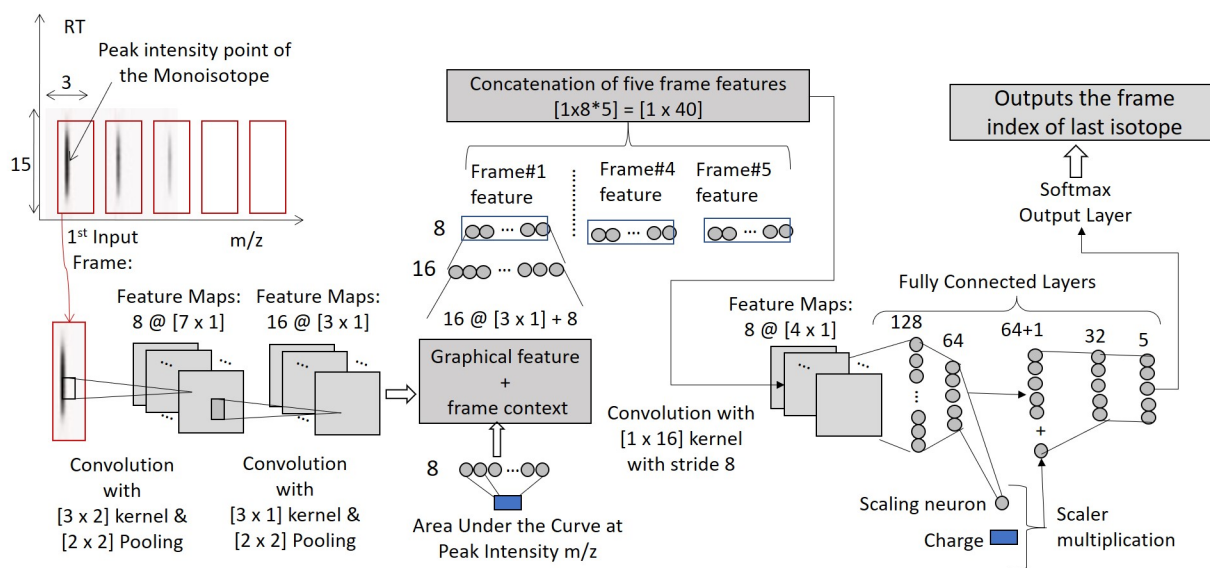


Figure 10. Network of IsoGrouping module. It starts with two convolution layers to fetch the graphical features from the input frame. Then we concatenate the total intensity (AUC) of the isotopic signal with it through an embedding layer of neurons (frame context). Then this is passed through two fully connected layers having size 16 and 8. This gives us ‘frame feature’ of the input frame. We perform the same for five consecutive frames and then concatenate the ‘frame feature’ of those altogether. Then one layer of convolution is applied to detect combined feature from all the frames. The resultant features are passed through two fully connected layers (size 128 and 64) to decide whether this is a noise or potential feature. This probability is also used to activate a scaling neuron, that feeds the charge into the network through proper scaling. Scaled charge is concatenated with the latest layer output (size 64) and passed through two fully connected layers. Finally the Softmax output layer at the end classifies the sequence. We include pooling layers after first and second convolution layers. We apply ReLu activation function for the neurons. The dropout layers are included after each fully connected layers with dropout probability of 0.5. The other network parameters are mentioned in the figure.

or blank area. We also generate sequences that contain peptide feature, but the feature does not start at the first frame of the sequence. Those samples are labeled as ‘0’ as well. We do this to handle the cases where noisy traces are classified as isotopes by IsoDetecting module by mistake and thus clustered with the actual features in the intermediate step. We see the training and validation sensitivity in Table 9. For the training, we set minibatch size 128 and apply ‘Adagrad’ stochastic optimization²⁹ with initial learning rate of 0.07. We use softmax cross entropy as error function at the output layer.

Class	Sensitivity on Training Set (%)	Sensitivity on Validation Set (%)
0 (noise)	89.42	90.78
1 (2 isotopes)	57.93	57.50
2 (3 isotopes)	51.98	43.30
3 (4 isotopes)	61.90	59.86
4 (5 isotopes or more)	61.77	64.14

Table 9. Class sensitivity of IsoGrouping module on training set and validation set. The output is $i = 0$ to 4, where, $i = 0$ means that no feature starts in the first frame, so skip it. Output $i = 1$ to 4 means, there is a feature starting in the first frame, and it ends at $(i + 1)^{th}$ frame. When output $i = 4$, it means there might be more isotopes left. So we run another round of processing over the rest of the isotopes of the same cluster or sequence. So although our network process 5 frames at a time, but if the feature has more than 5 isotopes, those can be found by overlapping rounds.

We observe that the maximum sensitivity of the classes is about 60%. To have a better perception we present the confusion matrix in Table 10. We see the model hardly misses the monoisotopes (low percentage of features misclassified as class A), but confuses about the last isotope of a peptide feature. Please note that reporting the monoisotope along with first few isotopes (having higher intensity peaks) of a feature is more important in the workflow. Because they dominate the feature intensity and used in the next steps of protein quantification and identification.

Class	0	1	2	3	4
0	89.43%	6.88%	1.72%	0.94%	1.03%
1	17.29%	57.93%	18.18%	5.58%	1.03%
2	5.38%	18.94%	51.98%	21.58%	2.13%
3	3.25%	5.44%	14.29%	61.90%	15.12%
4	5.71%	2.55%	3.18%	26.79%	61.77%

Table 10. Confusion matrix produced by IsoGrouping module on validation dataset. The diagonal values, e.g. [2, 2] represent the sensitivity for class 2. We say a feature is misclassified as class 0 when the monoisotope (first isotope) or all of the isotopes are missed, i.e., the feature is thought to be noise by mistake. The value of [2, 0] indicates what percentage of features with three isotopes are either misclassified as noise, or monoisotope is missed. [2, 1] indicates the percentage of features which actually have three isotopes but the third one is missed, and only first two are combined together. Similarly [2,3] shows for what percentage of three isotope features, IsoGrouping module finds ONE additional isotope at the end.

Finally, we would like to mention some common strategies followed for implementing and training both of the modules. We implemented our deep learning model using the Google developed Tensorflow library. We check the accuracy on validation set after training on every 1200 samples. We perform data shuffling after each epoch which helps to achieve convergence faster. We continue training until no progress is seen on validation set for about 15 epochs. For developing the PointIso we use Intel(R) Xeon(R) Gold 6134 CPU, NVIDIA Tesla GPU, and Ubuntu 16.04.5 LTS operating system.

Data Availability

The benchmark dataset is available to download from ProteomeXchange using accession number PXD001091. The full experimental result on all the replicates of the samples are available in supplementary materials. Source code can be found at this address: <https://github.com/anne04/PointIso>

References

1. LeCun, Y., Bengio, Y. & Hinton, G. Deep learning. *nature* **521**, 436 (2015).
2. Jaffe, J. D. *et al.* Pepper, a platform for experimental proteomic pattern recognition. *Mol. & Cell. Proteomics* **5**, 1927–1941 (2006).
3. Tran, N. H. *et al.* Complete de novo assembly of monoclonal antibody sequences. *Sci. reports* **6** (2016).
4. Bulik-Sullivan, B. *et al.* Deep learning using tumor hla peptide mass spectrometry datasets improves neoantigen identification. *Nat. biotechnology* **37**, 55 (2019).
5. Aoshima, K. *et al.* A simple peak detection and label-free quantitation algorithm for chromatography-mass spectrometry. *BMC bioinformatics* **15**, 376 (2014).
6. Tran, N. H. *et al.* Deep learning enables de novo peptide sequencing from data-independent-acquisition mass spectrometry. *Nat. methods* **16**, 63–66 (2019).
7. Gessulat, S. *et al.* Prosit: proteome-wide prediction of peptide tandem mass spectra by deep learning. *Nat. methods* **16**, 509 (2019).
8. Guan, S., Moran, M. F. & Ma, B. Prediction of lc-ms/ms properties of peptides from sequence by deep learning. *Mol. & Cell. Proteomics* **18**, 2099–2107 (2019).
9. Senior, A. W. *et al.* Improved protein structure prediction using potentials from deep learning. *Nature* 1–5 (2020).
10. Zohora, F. T. *et al.* Deepiso: A deep learning model for peptide feature detection from lc-ms map. *Sci. reports* **9**, 1–13 (2019).
11. Aebersold, R. & Mann, M. Mass spectrometry-based proteomics. *Nature* **422**, 198 (2003).
12. Steen, H. & Mann, M. The abc's (and xyz's) of peptide sequencing. *Nat. reviews. Mol. cell biology* **5**, 699 (2004).
13. Qi, C. R., Su, H., Mo, K. & Guibas, L. J. Pointnet: Deep learning on point sets for 3d classification and segmentation. In *Proceedings of the IEEE Conference on Computer Vision and Pattern Recognition*, 652–660 (2017).
14. Fu, J. *et al.* Dual attention network for scene segmentation. In *Proceedings of the IEEE Conference on Computer Vision and Pattern Recognition*, 3146–3154 (2019).

15. Chawade, A., Sandin, M., Teleman, J., Malmström, J. & Levander, F. Data processing has major impact on the outcome of quantitative label-free lc-ms analysis. *J. proteome research* **14**, 676–687 (2014).
16. Teleman, J. *et al.* Automated selected reaction monitoring software for accurate label-free protein quantification. *J. proteome research* **11**, 3766–3773 (2012).
17. Tautenhahn, R., Boettcher, C. & Neumann, S. Highly sensitive feature detection for high resolution lc/ms. *BMC bioinformatics* **9**, 504 (2008).
18. Kuncheva, L. I. *Combining pattern classifiers: methods and algorithms* (John Wiley & Sons, 2004).
19. Sturm, M. *et al.* Openms—an open-source software framework for mass spectrometry. *BMC bioinformatics* **9**, 163 (2008).
20. Röst, H. L. *et al.* Openms: a flexible open-source software platform for mass spectrometry data analysis. *Nat. methods* **13**, 741 (2016).
21. Cox, J. & Mann, M. Maxquant enables high peptide identification rates, individualized ppb-range mass accuracies and proteome-wide protein quantification. *Nat. biotechnology* **26**, 1367–1372 (2008).
22. Teleman, J., Chawade, A., Sandin, M., Levander, F. & Malmström, J. Dinosaur: a refined open-source peptide ms feature detector. *J. proteome research* **15**, 2143–2151 (2016).
23. Ma, B. *et al.* Peaks: powerful software for peptide de novo sequencing by tandem mass spectrometry. *Rapid communications mass spectrometry* **17**, 2337–2342 (2003).
24. Röst, H. L., Schmitt, U., Aebersold, R. & Malmström, L. pyopenms: a python-based interface to the openms mass-spectrometry algorithm library. *Proteomics* **14**, 74–77 (2014).
25. Michalski, A., Cox, J. & Mann, M. More than 100,000 detectable peptide species elute in single shotgun proteomics runs but the majority is inaccessible to data-dependent lc- ms/ms. *J. proteome research* **10**, 1785–1793 (2011).
26. Qiao, R. *et al.* Deepnovov2: Better de novo peptide sequencing with deep learning. *arXiv preprint arXiv:1904.08514* (2019).
27. Chambers, M. C. *et al.* A cross-platform toolkit for mass spectrometry and proteomics. *Nat. biotechnology* **30**, 918 (2012).
28. Kingma, D. & Ba, J. Adam: A method for stochastic optimization. *arXiv preprint arXiv:1412.6980* (2014).
29. Duchi, J., Hazan, E. & Singer, Y. Adaptive subgradient methods for online learning and stochastic optimization. *J. Mach. Learn. Res.* **12**, 2121–2159 (2011).

Acknowledgements

This work is partially supported by NSERC OGP0046506, NSF China grant 61832019, Canada Research Chair Program, The National Key R&D Program of China 2018YFB1003202, and Bioinformatics Solutions Inc. We thank Rui Qiao, Department of Statistics and Actuarial Science, University of Waterloo, Waterloo, ON, Canada, for sharing his thoughtful ideas about PointNet and class imbalance problems.

Author contributions

F.T.Z designed and developed the model, and performed the experiments as well. M.Z.R helped with producing database search result by MASCOT and setting parameters of other existing tools. M.Z.R. and L.X. helped with studying the characteristics of peptide features and LC-MS map. N.H.T contributed by suggesting various deep learning ideas. B.S. and M.L. proposed and supervised the project. All authors reviewed the manuscript.

Competing interests

The authors declare no competing interests.

PointIso: Point Cloud Based Deep Learning Model for Detecting Arbitrary-Precision Peptide Features in LC-MS Map through Attention Based Segmentation

Fatema Tuz Zohora, M Ziaur Rahman, Ngoc Hieu Tran, Lei Xin, Baozhen Shan, Ming Li

Supplementary Note A

Experiment Category	$z=0$	$z=1$	$z=2$	$z=3$	$z=4$
Without any class weight (after 10 epochs)	96%	40%	53%	33%	15%
Class weight based on distribution over whole dataset (after 10 epochs)	91%	48%	68%	51%	27%
Class weight based on distribution over sample (after 10 epochs)	86%	51%	71%	55%	30%
Same as above, after convergence	64%	59%	79%	67%	14%
Same as above, with attention mechanism	50%	79%	95%	91%	85%
Same as above, with attention mechanism and higher resolution	40%	99%	98%	98%	98%

Supplementary Table S 11. Class sensitivity for different weighting mechanisms. We compare the candidate weighting mechanisms based on the sensitivity for the best case scenario, i.e., when feature is aligned with the left boundary of the scanning window (e.g., feature A in Figure 4(a)), with high abundant features, i.e., features having charge, $z = 1, 2, 3, 4$. Please note that, although the sensitivity of negative class ($z=0$) is comparatively lower for our chosen criteria, however, it does not imply that it reports many false positives. Although the datapoints which are very close or adjacent to the real signal, are sometimes predicted as positive points, but in general the negative class has higher class sensitivity than all others as presented in Table 7 of the main manuscript.

Class Weight Assignment Procedure

We choose the class weight based on distribution per sample. Let us have a sample window which contains 100 datapoints. They come from three different classes (z): 0, 2, and 3. We have 10 points from $z = 3$, 30 points from $z = 2$, and remaining 60 points from $z = 0$. Then points from class 0, 2, and 3 get weights of 0.4, 0.7, and 0.9 respectively. We perform this for every sample. So every training sample has a weight list associated with it, which we pass to the network during cross entropy loss calculation.

Supplementary Note B

Attention Mechanism

We would like to discuss our experiments to correctly segment partially covered peptide features in a target window. We started with considering a bigger scanning window which will produce output for the center region. This caused three problems. First, we can apply back-propagation based on full bigger window during training time (number of input nodes equals to the number of output nodes), but use the center region only during testing time or prediction (output nodes corresponding to center region are used only). In this case model gets confused about the boundary region during training and cannot learn well. Second, during training time we can apply back-propagation based on center region only, therefore, number of input nodes is not equal to the number of output nodes anymore. This actually makes the architecture very complex. Because number of datapoints in the center region, and surrounding r_1, r_2, r_3, r_4 regions is never fixed. Although we consider a fixed number and do padding for simplification, but when number of input is not equal to the number of outputs, internal design gets quite complicated. Also the fact that, datapoints in r_1, r_2, r_3, r_4 need not to worry about each other, only have to focus on center region, may not be well learned by the model. We would not have any control over that. Finally, we also face technical issues since GPU memory exceeded (more than 16 GB) with bigger region. Because of these reasons we were unable to proceed with the design.

So we applied next simpler technique, sliding windows with 50% overlapping. The resultant class sensitivities are presented in the first row of Table S12. After passing the IsoDetecting output through IsoGrouping module, it finally produce only 65% feature detection as presented in the first row of Table 5. Therefore we had to use more sophisticated approach to address this problem.

In Figure 4 of main manuscript, we see that the regions r_1, r_2, r_3 , and r_4 are actually playing the key role in detecting the traces inside target window. We empirically tested following three techniques for diffusing the surrounding information into current window, and the results are summarized in Table S12.

Experiment Category	z=0	z=1	z=2	z=3	z=4
Sliding window with 50% overlapping	86%	50%	72%	57%	36%
Skiplink inserted in above model	85%	56%	76%	66%	41%
Bi-directional 2D RNN	85%	51%	77%	67%	49%
Attention mechanism	84%	62%	85%	71%	50%
Attention mechanism with higher resolution	90%	64%	85%	81%	61%

Supplementary Table S 12. Different techniques of absorbing surrounding information and corresponding class sensitivity of IsoDetecting module. We define the class sensitivity of a scanning window as the number of datapoints from class z (0 to 9) detected correctly out of total number of datapoints in a scanning window. To evaluate candidate solutions we use the class sensitivity of high abundant features (charge $z = 1, 2, 3$, and 4) in a *average case* scenario. Average case means the scanning window might contain any number of features, they may appear at any location of the window, they might be partially or fully seen, and might be overlapping as well. We see that the DANet inspired attention based mechanism works better than other techniques.

- First, we just calculated the global features of surrounding regions and diffuse them together by addition and concatenation with the global features of target window. Then we repeated the 50% overlapping technique, which did not bring any significant change. Using some skip links along with that brings little improvement as shown in the second row of the table.
- Then we used a bi-directional two dimensional RNN network to flow information from all direction into the target window. The corresponding class sensitivities are provided in the third row.
- Finally, we applied the attention mechanism proposed by DANet which works better than first two techniques, as reported in the fourth and fifth row. So we choose PointNet segmentation network combined with DANet to develop our IsoDetecting module.

Supplementary Note C

Controlling False Detection Rate

The secondary signals very close to the primary signals are usually merged with the primary signal through some pre-processing which involves different parameter settings based on dataset and context. However, we tend to avoid all kind of heuristic parameters and therefore work on raw LC-MS map. That is why our algorithm has to perform noise removal as well as feature detection. Although random noise removal is learned easily by PointIso but separation of feature like noisy traces and those secondary peaks removal is difficult for PointIso. This tasks has to be performed by IsoDetecting module since it has the access to whole context. So it has to see through all the signals and decide which ones are to be reported and which are to be ignored. Our initial trained model reports those feature like signals as peptide features. Therefore we fine tune the model to resolve this problem.

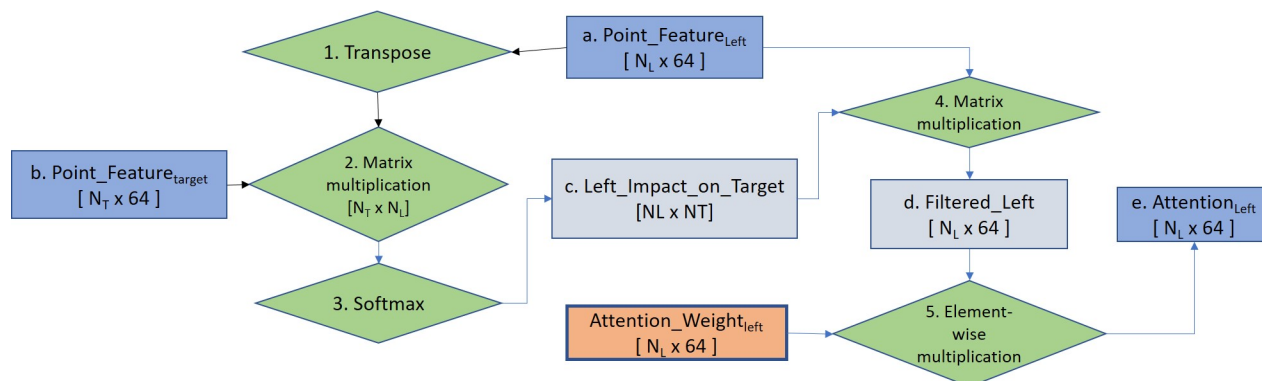
In order to do collect those wrong reports, we first let our model scan through a LC-MS map and report peptide feature list. Then we match that list with the peptide feature list produced by all other tools (i.e., OpenMS, MaxQuant, Dinosaurs, and PEAKS) with an error tolerance of $0.01m/z$ and 0.2 min RT. The features from PointIso list which did not match are selected for fine tuning (about 70,000 features). We cut those features' corresponding scanning window along with surrounding region, as done for other training samples. Then we start with already trained model, run few epochs with 0.0001 learning rate and keep the best model state. We use about 30,000 samples for fine tuning. We can balance between the true detection rate and false detection rate using the amount of these samples.

This same set of features can be also used for fine tuning IsoGrouping module. But its not very effective since it sees only filtered out signals and does not have access to the bigger context like IsoDetecting module. We save two types of model state while training the IsoGrouping module. One is best loss model, and another is best sensitivity model based on validation dataset. Best loss model gives us lower number of peptide features then the best sensitivity model, however, detection percentage is also dropped a little bit. For example, we get 97.53% detection with 80,000 features, instead of 98.06% detection with 100,000 features (which is reported in the main result). Without any fine tuning we get 99.50% detection, with about 200,000 features.

In our manuscript we have used fine tuned model of IsoDetecting module, and best sensitivity model of IsoGrouping module. But the other models are also uploaded in the GitHub repository. Users can choose according to their need. They can also fine tune further if necessary.

Supplementary Method A

Attention Calculation



Supplementary Figure S 11. Flowchart of attention calculation in IsoDetecting module. This particular flowchart is intended to find out the attention or impact of left region over the datapoints of target window. Exactly similar approach is followed for other surrounding regions as well and finally all are diffused with the *point_features_target* by addition.

Please refer to the flowchart shown in Figure 11. We have the point features of left region, *point_feature_left* according to the PointNet architecture shown in the main manuscript. Then we multiply *point_feature_target* with the transpose of *point_feature_left* according to the rule of matrix multiplication. Then we take softmax of the product as Equation 1, which gives us a $[N_T \times N_L]$ matrix, *left_impact_on_target*, where, N_T and N_L are the total number of datapoints of the target window and left region respectively. So each row presents a datapoint from target window and columns present the datapoints from left region.

$$left_impact_on_target = \frac{\exp((point_feature_target_i) \cdot (point_feature_left_j))}{\sum_{i=1}^{N_L} \exp((point_feature_target_i) \cdot (point_feature_left_j))} \quad (1)$$

Therefore, *left_impact_on_target*_(j,i) presents the attention of i^{th} point of left region over the j^{th} point of target window. The higher the value, the higher the correlation (similar feature) between those two points. So the j^{th} row tells us which datapoints from left region have higher attention or highly correlated with the j^{th} datapoint of target window. Next, we want to fetch those *significant point features from left region. So we apply another round of matrix multiplication (4th operation) between *left_impact_on_target* and *point_feature_left*. We denote the resultant product as *filtered_left* since it essentially gives us *point_features_left* but scaled/filtered according to the aforementioned correlation or attention. Then again we have to know how much of those filtered features should be incorporated with the *point_features_target* while segmenting the datapoints of target window. So we use a weight matrices, namely *Attention_Weight_left*, and multiply it with *filtered_left*, producing *attention_left*, which is finally passed forward to be diffused (by addition) with the *point_features_target*. This *Attention_Weight_left* is learned through training.

Supplementary Note D

Basic Properties of Peptide Feature

It is supposed to learn following basic properties of peptide feature, besides many other hidden characteristics from the training data.

1. In the LC-MS map, the isotopes in a peptide feature are equidistant along m/z axis. For charge $z = 1$ to 9, the isotopes are respectively $1.00 m/z$, $0.5 m/z$, $0.33 m/z$, $0.25 m/z$, $0.17 m/z$, $0.14 m/z$, $0.13 m/z$, and $0.19 m/z$ distance apart from each other¹².
2. The intensities of the isotopes form bell shape within their retention time (RT) range as shown in the zoomed in view of Figure 1 of the main manuscript.
3. Peptide features often overlap with each other.

Supplementary Method B

Resolution Degradation in IsoGrouping Module

IsoDetecting module generates sequences of potential isotopes which are sent to the IsoGrouping module for final detection of peptide features. Now, the m/z value of isotopic signals are real numbers having up to 4 decimal places. We degrade each signal into real numbers having up to 2 decimal places. For example, let us have two sequences of isotopes A , and B , where the first isotope of the sequences are denoted as A_1 and B_1 respectively. The m/z values of these are respectively $A_{1_mz} = 500.2351$ and $B_{1_mz} = 500.2443$. During resolution degradation we filter out the signal intensity from the background with ± 2 ppm m/z range. The range is calculated as: $\frac{A_{1_mz} \times 2.0}{10^6}$. So that we have $A_{1_mz} = 500.24$ and intensity is set as the maximum of the intensities of datapoints within range 500.2341 to 500.2361. Similarly, $B_{1_mz} = 500.24$, *but* intensity is set as the maximum of the intensities of datapoints within range 500.2433 to 500.2453. So we see that, although both have the same m/z values in lower resolution, they definitely belong to different sequences and have different intensities (thus might have different pattern as well).

Supplementary Method C

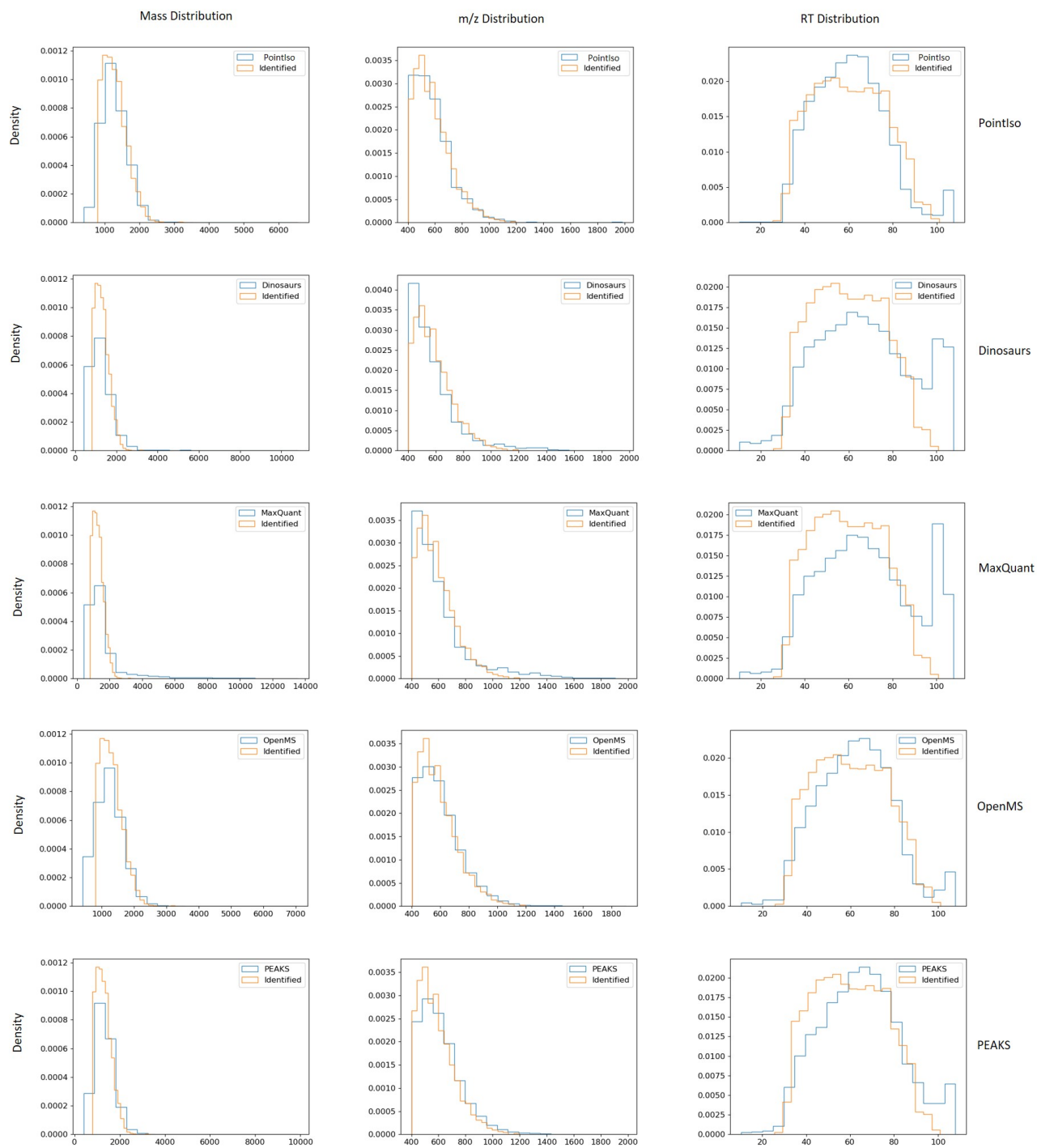
Scanning Procedure by IsoGrouping Module

This method is intentionally kept similar to DeepIso. Although we have upgraded the internal architecture significantly, for the sake of user convenience we do not change the scanning procedure. Therefore, we request our readers to refer to the corresponding material from DeepIso.

Supplementary Table S3: Percentage of identified peptide features by different algorithms					
LC-MS maps	OpenMS	MaxQuant	Dinosaurs	DeepIsoV2	Peaks
130124_dilA_1_01	94.2266	94.6575	95.4761	98.0181	95.6053
130124_dilA_1_02	96.0611	94.8955	95.4582	98.8344	95.8601
130124_dilA_1_03	95.9013	95.3994	95.8176	98.2016	96.0686
130124_dilA_1_04	95.444	95.1351	95.444	98.1467	95.5598
	95.40825	95.021875	95.548975	98.3002	95.7735
130124_dilA_2_01	96.3771	95.2163	96.2012	98.593	95.7088
130124_dilA_2_02	95.6753	95.5335	96.1361	98.3339	95.6044
130124_dilA_2_03	96.107	94.9221	95.9039	99.0521	95.7346
130124_dilA_2_04	95.8291	94.9135	95.6256	98.4401	78.942
130124_dilA_2_05	96.0703	95.0362	95.6222	98.1041	95.5188
130124_dilA_2_06	95.7873	94.6133	95.8564	98.308	95.442
130124_dilA_2_07	96.2179	95.7668	95.975	98.3692	95.8362
	96.00914286	95.1431	95.90291429	98.4572	93.2553
130124_dilA_3_01	95.9933	95.3872	96.2963	98.3838	95.9933
130124_dilA_3_02	96.3699	95.6849	96.4041	98.6301	96.3014
130124_dilA_3_03	96.0927	95.596	96.8212	98.543	96.6225
130124_dilA_3_04	96.1678	95.0446	95.9035	99.0089	95.9035
130124_dilA_3_05	95.9974	95.7392	96.417	98.5474	96.3525
130124_dilA_3_06	96.5644	95.497	96.5977	98.0654	96.0974
130124_dilA_3_07	96.3929	95.5556	95.942	98.0998	96.1997
	96.22548571	95.50064286	96.34025714	98.46834286	96.21
130124_dilA_4_01	96.3514	95.6784	96.3868	98.1226	96.3868
130124_dilA_4_02	95.8527	95.3522	95.6382	97.4973	96.2817
130124_dilA_4_03	96.286	96.286	96.7025	98.2645	96.772
130124_dilA_4_04	96.011	95.4952	96.4237	98.7276	96.2173
130124_dilA_4_05	96.3086	95.5437	96.1756	98.9691	96.0758
130124_dilA_4_06	96.4737	95.5755	96.6401	98.4365	96.3407
130124_dilA_4_07	97.3072	96.0771	97.0412	98.1383	96.5426

	96.37008571	95.71544286	96.42972857	98.30798571	96.3738
130124_dilA_5_01	95.6699	95.6699	96.151	97.9645	96.225
130124_dilA_5_02	95.747	95.8899	96.2831	98.0343	96.1401
130124_dilA_5_03	96.3406	95.3488	96.3748	97.777	96.4774
130124_dilA_5_04	96.1288	94.9298	96.026	98.9723	95.9918
	95.971575	95.4596	96.208725	98.187025	96.2086
130124_dilA_6_01	96.4139	96.1524	96.6007	97.5719	96.526
130124_dilA_6_02	96.0598	95.3667	96.1328	98.5042	96.1693
130124_dilA_6_03	96.3015	95.28	95.8084	98.3093	95.7027
130124_dilA_6_04	95.321	95.2186	95.8333	97.4044	95.4918
	96.02405	95.504425	96.0938	97.94745	95.9724
130124_dilA_7_01	95.4466	94.7167	95.4814	98.1578	95.1338
130124_dilA_7_02	96.1326	95.9254	96.6851	98.9986	95.9945
130124_dilA_7_03	95.9586	95.0568	96.0254	98.664	95.992
130124_dilA_7_04	95.7404	94.929	95.9094	97.7688	95.6051
	95.81955	95.156975	96.025325	98.3973	95.6814
130124_dilA_8_01	95.9857	95.4122	96.0573	97.957	95.6631
130124_dilA_8_02	95.8304	94.7703	95.4417	97.7739	95.689
130124_dilA_8_03	95.9361	95.3803	96.3876	98.2633	96.1445
130124_dilA_8_04	95.7613	95.3204	96.0665	98.2028	95.9986
	95.878375	95.2208	95.988275	98.04925	95.8738
130124_dilA_9_01	95.604	94.8282	95.9365	98.7071	95.4932
130124_dilA_9_02	96.3676	95.5685	96.6945	98.1475	96.5492
130124_dilA_9_03	95.5315	95.1712	96.036	97.9459	95.6396
130124_dilA_9_04	96.2108	95.453	96.3142	98.5188	95.8663
	95.928475	95.255225	96.2453	98.329825	95.8871
130124_dilA_10_01	95.3586	95.2436	96.0491	98.3122	95.8189
130124_dilA_10_02	94.8629	95.3418	96.5607	96.8219	96.3431
130124_dilA_10_03	95.7868	95.1026	95.7148	97.8394	95.9309
130124_dilA_10_04	96.4209	95.4903	96.3135	98.5326	96.4209
	95.6073	95.294575	96.159525	97.876525	96.1284

130124_dilA_11_01	96.0899	95.3411	95.9651	98.4193	95.7155
130124_dilA_11_02	95.2318	95.2759	96.0706	95.9382	95.4525
130124_dilA_11_03	95.5888	95.1311	95.4224	97.0037	95.5472
130124_dilA_11_04	95.5084	94.7325	95.0592	98.1625	95.3042
	95.604725	95.12015	95.629325	97.380925	95.5049
130124_dilA_12_01	95.0474	94.3625	95.2582	95.8377	94.8894
130124_dilA_12_02	95.7128	94.7481	95.7128	95.9271	94.8553
130124_dilA_12_03	95.7011	94.5752	95.6499	96.4176	95.5476
130124_dilA_12_04	95.3646	94.4271	95.4167	97.3958	95
	95.456475	94.528225	95.5094	96.39455	95.0731
1	95.40825	95.021875	95.548975	98.3002	95.7735
2	96.00914286	95.1431	95.90291429	98.4572	93.2553
3	96.22548571	95.50064286	96.34025714	98.46834286	96.21
4	96.37008571	95.71544286	96.42972857	98.30798571	96.3738
5	95.971575	95.4596	96.208725	98.187025	96.2086
6	96.02405	95.504425	96.0938	97.94745	95.9724
7	95.81955	95.156975	96.025325	98.3973	95.6814
8	95.878375	95.2208	95.988275	98.04925	95.8738
9	95.928475	95.255225	96.2453	98.329825	95.8871
10	95.6073	95.294575	96.159525	97.876525	96.1284
11	95.604725	95.12015	95.629325	97.380925	95.5049
12	95.456475	94.528225	95.5094	96.39455	95.0731
average	95.85862411	95.24341964	96.00679583	98.00804821	95.66185833



Supplementary Figure S 12. Comparison of mass, m/z and RT distribution of detected features (blue) and identified features (orange) for different tools.